Cell Host & Microbe
Article

# CYCLOPS, A DNA-Binding Transcriptional Activator, Orchestrates Symbiotic Root Nodule Development

Sylvia Singh,[1,2] Katja Katzer,[1,2] Jayne Lambert,[1] Marion Cerri,[1] and Martin Parniske[1,*]
[1]Faculty of Biology, Genetics, University of Munich (LMU), D-82152 Martinsried, Germany
[2]These authors contributed equally to this work
*Correspondence: parniske@lmu.de
http://dx.doi.org/10.1016/j.chom.2014.01.011

## SUMMARY

**Nuclear calcium oscillations are a hallmark of symbiotically stimulated plant root cells. Activation of the central nuclear decoder, calcium- and calmodulin-dependent kinase (CCaMK), triggers the entire symbiotic program including root nodule organogenesis, but the mechanism of signal transduction by CCaMK was unknown. We show that CYCLOPS, a direct phosphorylation substrate of CCaMK, is a DNA-binding transcriptional activator. Two phosphorylated serine residues within the N-terminal negative regulatory domain of CYCLOPS are necessary for its activity. CYCLOPS binds DNA in a sequence-specific and phosphorylation-dependent manner and transactivates the *NODULE INCEPTION* (*NIN*) gene. A phosphomimetic version of CYCLOPS was sufficient to trigger root nodule organogenesis in the absence of rhizobia and CCaMK. CYCLOPS thus induces a transcriptional activation cascade, in which NIN and a heterotrimeric NF-Y complex act in hierarchical succession to initiate symbiotic root nodule development.**

## INTRODUCTION

A striking feature of symbiosis between legume plants and rhizobia is the development of a new plant organ, the root nodule. Upon symbiotic stimulation, a differentiated, resting root cell completely reprograms and either enters cell division to initiate nodule organogenesis or develops an intracellular structure for the accommodation of microsymbionts (Gutjahr and Parniske, 2013). The establishment of root symbioses between phosphate-acquiring arbuscular mycorrhiza (AM) fungi and the majority of land plants or between nitrogen-fixing rhizobia and legumes is initiated by an ancient signal transduction system (Oldroyd, 2013). The perception of symbiont-specific AM fungal factors or rhizobia-derived nodulation factors (“nod factors”) via cognate transmembrane receptors leads within minutes to the generation of sustained oscillations of calcium concentration (“calcium-spiking”) in the nucleus, a hallmark of symbiotic signal transduction (Ehrhardt et al., 1996; Oldroyd, 2013). In mammals, stimulus-dependent elevations of nuclear calcium concentration have been linked to changes in transcription, resulting in cell proliferation and growth (Bootman et al., 2009). Similarly, during plant root symbiosis, nuclear calcium spiking is believed to activate, in a hitherto unknown manner, the expression of symbiosis-associated genes (Miwa et al., 2006).

The nuclear calcium- and calmodulin-dependent kinase CCaMK is the central regulator of symbiotic development of the root (Singh and Parniske, 2012). A calmodulin (CaM) binding domain and three calcium-binding EF hands in CCaMK mediate regulation by calcium signatures (Swainsbury et al., 2012). *ccamk* mutants are completely symbiosis deficient. Rhizobia do not induce nodule organogenesis or infection threads and arbuscules, highly branched fungal structures within plant cells that are the site of symbiotic nutrient exchange, do not form upon inoculation with AM fungi (Lévy et al., 2004; Mitra et al., 2004). Importantly, autoactive CCaMK versions carrying various amino acid substitutions in the regulatory autophosphorylation site (T265D or T265I) can compensate for the loss of upstream genes involved in calcium-spike generation, consistent with the idea that the primary function of calcium spiking is the activation of CCaMK (Hayashi et al., 2010; Madsen et al., 2010). Deregulated CCaMK versions trigger the development of root nodules in the absence of external symbiotic stimuli demonstrating that CCaMK acts as central regulator of this developmental program (Gleason et al., 2006; Tirichine et al., 2006).

Root nodule organogenesis is initiated by cell divisions in the inner cortex (Oldroyd, 2013) and depends on the GRAS proteins Nodulation Signaling Pathway1 (NSP1) and NSP2 and the transcriptional regulator NODULE INCEPTION (NIN) (Kaló et al., 2005; Schauser et al., 1999; Smit et al., 2005). A relatively high hierarchical position of *NIN* in the initiation of lateral root organs is indicated by the observation that NIN targets the promoters of two subunits of the heterotrimeric CCAAT-box binding Nuclear Factor Y (NF-Y) complex: NF-YA1 and NF-YB1 (Soyano et al., 2013). Furthermore, ectopic overexpression of *NIN* or *NF-YA1* stimulated cell divisions resulting in the formation of aberrant lateral root organs that differed morphologically from both roots and nodules (Soyano et al., 2013).

Despite the central importance of CCaMK as a decoder of calcium-spiking and NIN as a mediator of organogenesis, the connection between CCaMK and the activation of gene expression was unclear. Here we addressed this issue by investigating the function of CYCLOPS, a direct interactor of CCaMK. Since its identification as essential gene for symbiosis development, the molecular function of *CYCLOPS*, encoding a nuclear coiled-coil protein, remained enigmatic (Yano et al., 2008). CYCLOPS interacts with and is phosphorylated by CCaMK in vitro,

implicating CYCLOPS as direct CCaMK phosphorylation target, which could either directly or indirectly be involved in the transcriptional reprogramming that leads to reinitiation of cell division. *NIN* expression is rapidly induced after nod factor perception, but severely reduced in *cyclops* mutants (Yano et al., 2008). Although *cyclops* mutants are impaired in AM and root nodule symbiosis, they do not recapitulate the *ccamk* mutant phenotype. They respond to rhizobia with root hair curling, but infection is aborted at the root hair stage. Likewise, nodule primordia form, but nodule development is prematurely arrested (Yano et al., 2008).

Here we show that CYCLOPS is a CCaMK-regulated DNA-binding transcriptional activator that initiates gene expression leading to nodule organogenesis. Our data reveal a direct mechanism of nuclear calcium signal decoding by the CCaMK/CYCLOPS complex: Perception of calcium signals stimulates phosphorylation of CYCLOPS, which in turn activates gene expression sufficient for the initiation of cell division and symbiotic organ development.

## RESULTS

### CYCLOPS Is a Phosphorylation Substrate of CCaMK

We hypothesized that CCaMK-mediated CYCLOPS phosphorylation would be a consequence of nuclear calcium spiking and thus a potential intermediate transduction step in symbiosis signaling. CYCLOPS was strongly phosphorylated by CCaMK only in the presence of calcium/CaM (Figure S1A). We detected five phosphorylated serines by mass spectrometry, which were all preceded by an arginine at position −3, suggesting that the consensus sequence "RXXS" was a preferred phosphorylation motif of CCaMK (Figure S1B).

### The CYCLOPS Phosphorylation Sites S50 and S154 Are Essential for Symbiosis

To examine whether phosphorylation of the identified sites is essential for symbiosis, we generated single- and multisite phosphoablative mutant versions of S14, S50, S154, S251, and S412, by amino acid (aa) exchange to alanine (A) and analyzed restoration of symbiosis in transformed *cyclops-3* mutant roots (Table S1 and Figure S2). Alanine replacement of either S50 or S154 did not, but only the simultaneous replacement of both sites impaired CYCLOPS' function in symbiosis (Figure S2). If phosphorylation at these two residues was important, the corresponding phosphomimetic serine to aspartate (D) replacements may result in a gain-of-function activity of the protein. Indeed, individual replacements or the combination of S50D-S154D (*3xHA-gCYCLOPS-DD*) all restored symbiosis (Table S2). To address the relevance of the three remaining sites we transformed *cyclops-3* roots with $CYC_{pro}$*:3xHA-gCYCLOPS-A-DD-AA* (carrying replacements of S14, S251, and S412 by A) and found that symbiosis was restored (Table S2). In summary, phosphorylation of S14, S251, and S412 is dispensable in the triple mutant, while phosphorylation of CYCLOPS at either S50 or S154 appears to be a prerequisite for symbiotic development.

### The Phosphorylation Status of CYCLOPS Does Not Affect Complex Formation with CCaMK

Ablation of CYCLOPS phosphorylation at S50 and S154 impaired symbiosis. To unravel the mechanistic cause for the functional defect, we investigated the consequences for protein expression levels, subcellular localization, and complex formation with CCaMK. All tested CYCLOPS versions were abundantly expressed and, equivalent to the wild-type (WT) protein, localized exclusively to the nucleus (Figures S3A and S3B). Also, complex formation with CCaMK was not compromised and equally strong as demonstrated by fluorescence lifetime imaging microscopy (FLIM)-FRET measurements (Figures 1A–1F).

### The *NIN* Promoter Is Activated In *trans* by CYCLOPS in a Phosphorylation-Dependent Manner

Deregulated CCaMK is sufficient to induce symbiosis-related transcriptional reprogramming (Gleason et al., 2006; Tirichine et al., 2006). Since CYCLOPS is a phosphorylation target of CCaMK, the most parsimonious model implicated CYCLOPS directly in transcriptional regulation of target genes. To test this, a *NIN* promoter (>2 kb) fusion to the *uidA* gene (*pNIN:GUS*) was coexpressed together with *3xHA-CYCLOPS* and with or without autoactive *3xHA-CCaMK-T265D* in *N. benthamiana* leaf cells. CYCLOPS alone caused a faint reporter expression, while coexpression with CCaMK-T265D induced a significant increase (Figure 2A). CCaMK-T265D alone did not elicit *GUS* expression, indicating that the observed transactivation was not mediated by phosphorylation of endogenous proteins. This finding suggested that the increase in transactivation resulted from phosphorylation of CYCLOPS by CCaMK-T265D. To test whether phosphorylation of S50 and S154 is involved, we examined if this effect can be recapitulated or prevented by the phosphomimetic and phosphoablative versions, respectively. CYCLOPS-DD alone transactivated strongly, while CYCLOPS-AA alone or in combination with CCaMK-T265D did not (Figure 2A). In conclusion, CYCLOPS has properties of a transcriptional activator. Since the coexpression of CYCLOPS with autoactive CCaMK transactivated the *NIN* promoter and this effect was not observed with the phosphoablative version but was fully recapitulated with the phosphomimetic version alone, we concluded that phosphorylation at S50 and S154 is a likely mechanism of CYCLOPS activation.

### Identification of a CYCLOPS Responsive *Cis* Element (*CYC-RE*) within the *NIN* Promoter

We performed a detailed deletion and substitution analysis of the *NIN* promoter to identify *cis* elements targeted by CYCLOPS-DD (Figures 2B–2F). We delimited a CYCLOPS response element "*CYC-RE*" to a 30 bp fragment containing a palindromic sequence (Figure 2F). Substitution analysis pinpointed the palindrome as essential *cis* element, or "*CYC-box*" for CYCLOPS-DD-mediated *CYC-RE* reporter induction (Figure 2F).

### CYCLOPS-DD Binds DNA in a Sequence-Specific and Phosphorylation-Dependent Manner

To test direct binding of CYCLOPS-DD to DNA, electrophoretic mobility shift assays (EMSAs) were employed. CYCLOPS-DD caused a shift of IR-labeled *CYC-RE* probe, indicating protein-DNA interaction. Unlabeled *CYC-RE* DNA competed successfully for the binding, while mutated competitor DNA (*mCYC-RE*) did not (Figure 3A). This analysis demonstrated that CYCLOPS-DD has sequence-specific DNA binding properties. The sequence specificity was similar to that observed for

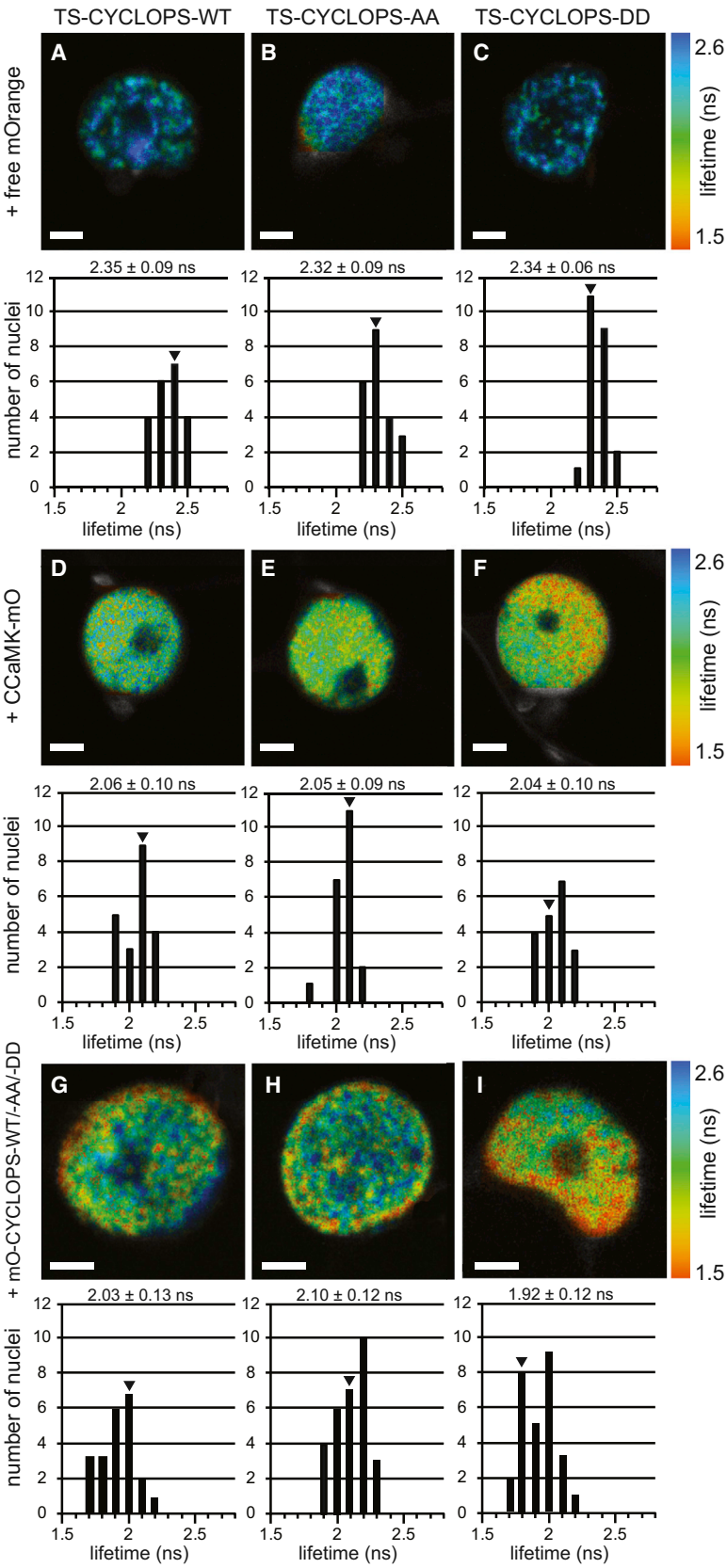


**Figure 1. CYCLOPS Interacts with CCaMK and Forms Homodimers**

(A–C) FLIM-FRET analysis of TSapphire-CYCLOPS (TS-CYCLOPS) and phosphosite mutants. In the presence of free mOrange (mO) no difference in fluorescent lifetimes (FLs) between CYCLOPS variants was observed (ANOVA $F_{2,63}$ = 0.701, p = 0.5).

(D–F) FLs were significantly reduced in the presence of CCaMK-mO, indicating interaction independent of the phosphosite substitution (D-F: no difference between CYCLOPS variants, ANOVA $F_{2,58}$ = 0.096, p = 0.908).

(G–I) Dimerization was detected for TS-CYCLOPS phosphosite variants with their respective mO-CYCLOPS partners with a significant difference between the CYCLOPS variants (ANOVA $F_{2,77}$ = 16.09, p = 1.45e-06). In detail, whereas the FL of TS-CYCLOPS-WT and TS-CYCLOPS-AA did not differ in the dimer assay (Tukey's HSD, p = 0.105), it was significantly shorter for TS-CYCLOPS-DD (Tukey's HSD p = 0.006, p = 0.8e-6 respectively).The FL of the TS donor fluorophore is depicted in a color code from blue (2.6 ns) to red (1.5 ns) for one representative nucleus per construct combination. Histograms below the images represent FLs of all nuclei analyzed; arrowheads indicate the FL classes of the depicted nuclei. Insets show mean values and standard deviations obtained per construct combination. Analysis was performed on nuclei of *N. benthamiana* leaf cells 60 hr post infiltration. Bars: 2 μm. See also Figures S1, S2, and S3.

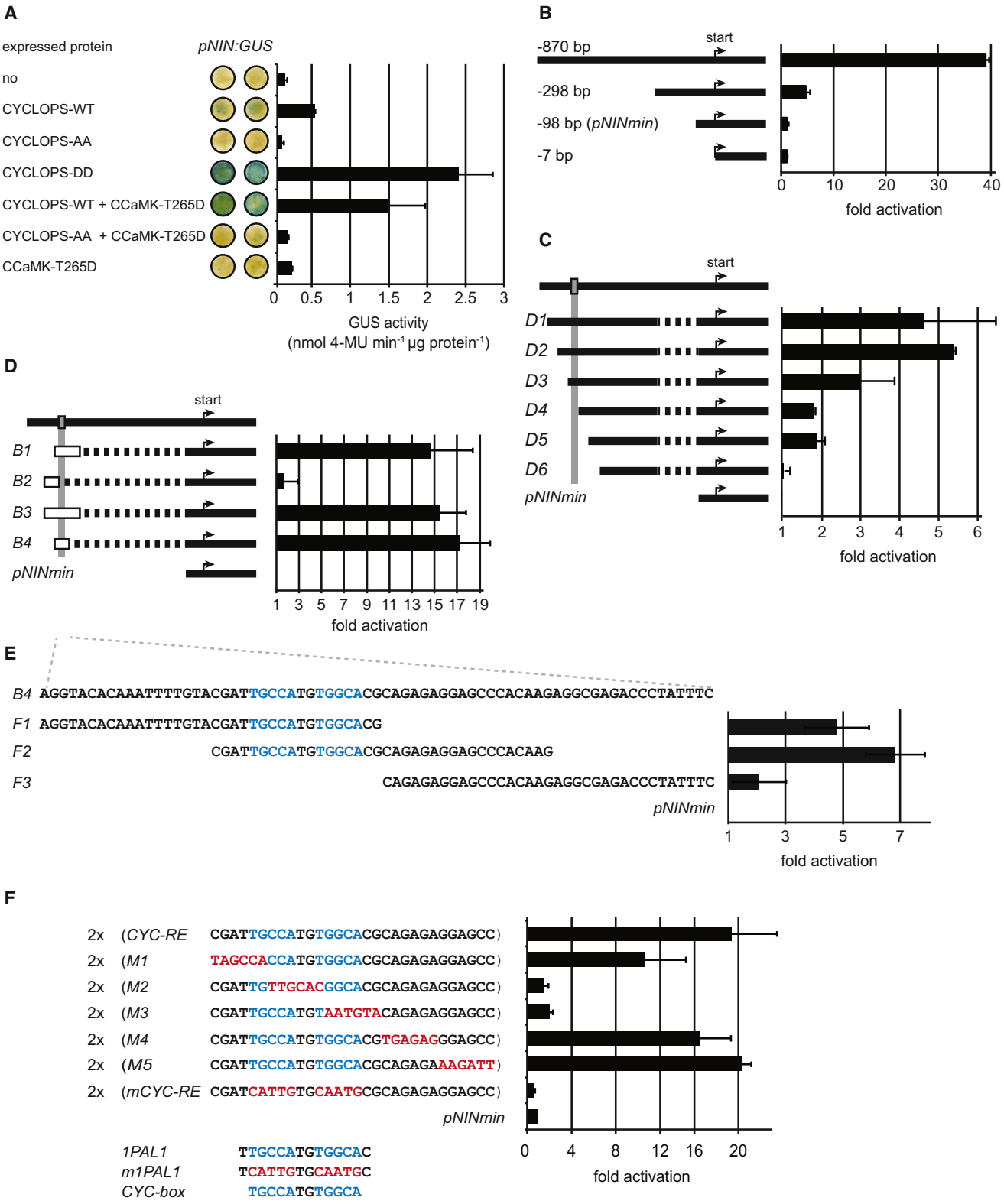


**Figure 2. CYCLOPS-DD Transactivates the *NIN* Promoter via a Palindromic *Cis* Element**

(A) Transactivation assay in *N. benthamiana* leaves showing that CYCLOPS-DD alone or CYCLOPS-WT coexpressed with autoactive CCaMK-T265D lead to transcriptional activation of the *NIN* promoter. *N. benthamiana* leaf cells were cotransformed with T-DNAs encoding the indicated *3xHA-CYCLOPS* variants and

*(legend continued on next page)*

the transcriptional activation by CYCLOPS-DD (Figure 2F). Further, 3xHA-CYCLOPS-DD also exhibited specific association with the *NIN* promoter in vivo (Figure S4). Taken together, these findings pinpoint direct DNA binding of CYCLOPS-DD as the most likely mechanism mediating sequence-specific transcriptional activation.

Coexpression of CYCLOPS with CCaMK in *E.coli* resulted in a strong phosphorylation of CYCLOPS, which was not observed when CYCLOPS was expressed alone (data not shown). To assess whether CYCLOPS binding to the *CYC-RE* was dependent on the phosphorylation state, CYCLOPS expressed with or without CCaMK was tested by EMSA. Only CYCLOPS-DD and the CYCLOPS-WT protein purified after coexpression with CCaMK bound to *CYC-RE*, while binding was not detected with CYCLOPS-WT and CYCLOPS-AA proteins expressed in the absence of CCaMK (Figure 3B, left panel). CCaMK alone caused no shift of the *CYC-RE* probe (data not shown). The bandshift induced by CCaMK-pretreated CYCLOPS-WT protein was lost after phosphatase treatment (Figure 3B, right panel). This finding is consistent with the idea that phosphorylation promotes CYCLOPS' DNA binding activity.

## CYCLOPS Forms Homodimers and Its Conformation Is Altered Upon Phosphomimetic Replacement of S50 and S154

The *CYC-box* contains a palindromic sequence, suggesting that CYCLOPS binds as a dimer. Consistent with this, we detected dimer formation of CYCLOPS by BiFC (Figure S3C). By using FLIM-FRET, homodimer formation was detected for CYCLOPS-WT, CYCLOPS-AA, and the CYCLOPS-DD variants (Figures 1G–1I), suggesting that dimerization is independent of the phosphorylation state of the S50 and S154 residues. However, FLIM-FRET was significantly stronger with the CYCLOPS-DD version (Figure 1I) indicating a conformational change of the dimer induced by the phosphomimetic replacements. It is therefore possible that the conformational transitions induced by phosphorylation of CYCLOPS are responsible for the alterations in the DNA-binding properties of the dimer.

## CYCLOPS Is a Modular DNA-Binding Transcriptional Activator

As CYCLOPS exhibited DNA-binding and transcriptional activation properties, we aimed to assign these activities to distinct CYCLOPS domains. To detect and map the transcriptional activation domain of CYCLOPS ($AD_{CYC}$), fusions of the DNA-binding domain of the yeast Gal4 transcription factor ($BD_{Gal4}$) to the N terminus of 3xHA-CYCLOPS derivatives were tested in *N. benthamiana* for transactivation of the cognate reporter *p5xUAS$_{Gal4}$:eGFP-GUS$_{intron}$* (Figure 4A). $BD_{Gal4}$-3xHA-CYCLOPS-DD mediated strong transactivation, confirming the presence of an activation domain in CYCLOPS. The position of the $AD_{CYC}$ was narrowed down to aa 267–380, as this truncation conferred strong transactivation, while the N-terminal half of CYCLOPS-DD (aa 1–265) and the C-terminal domain (aa 364–518) did not (Figure 4A). Importantly, a tandem repeat fusion of $AD_{CYC}$ to the $BD_{Gal4}$ was able to trigger strong autoactivation in yeast, suggesting that $AD_{CYC}$ interacts with a conserved component of the basal transcription machinery, e.g., the mediator (Figure S5) (Conaway et al., 2005).

To identify CYCLOPS' DNA-binding domain ($BD_{CYC}$), fusions of the $AD_{VP16}$ to the N terminus of 3xHA-CYCLOPS derivatives were analyzed for their ability to activate a *2xCYC-RE:GUS* reporter in *N. benthamiana* (Figure 4B). An $AD_{VP16}$ fusion to the C-terminal half of CYCLOPS (aa 255–518) and a fusion to the C-terminal coiled-coil (aa 364–518) were both able to transactivate (Figure 4B) indicating that the $BD_{CYC}$ is located at the C terminus. Consistent with this, a deletion of the C-terminal coiled-coil (aa 1–449) led to the loss of transactivation (Figure 4B).

Since the $BD_{CYC}$ and $AD_{CYC}$ were located in the C-terminal half of the protein, we tested whether a minimal CYCLOPS version ("CYCLOPS-min", aa 255–518) was sufficient to mediate DNA binding and transcriptional activation (Figures 4A and 4B). Indeed, CYCLOPS-min transactivated the *2xCYC-RE:GUS* reporter in *N. benthamiana* and *L. japonicus* (Figures 4C and 4F) with a sequence-specificity matching that of CYCLOPS-DD (Figure 4C). This finding is in line with the idea that the deleted N terminus, which also contains the two critical phosphorylation sites, is a negative regulatory domain of CYCLOPS.

the *pNIN:GUS* reporter, with or without *3xHA-CCaMK-T265D*. GUS activity was determined histochemically and quantitatively in leaf discs. Mean values and standard deviations were determined from three biological replicates. Photographs of leaf discs represent two biological replicates.

(B–F) Identification of a CYCLOPS-DD responsive *cis* element (*CYC-RE*; shaded in gray in C and D) within the *NIN* promoter. The indicated *NIN* promoter fragments fused to the *GUS* reporter gene were coexpressed with *3xHA-CYCLOPS-DD* in *N. benthamiana* leaf cells. Mean value of GUS activity and standard deviation from three biological replicates is given for each promoter construct. The *NIN* promoter length is annotated from the transcriptional start site (start). In (B), rough mapping identified at least two CYCLOPS-DD response elements (RE) in the intervals from −870 to −299 bp and from −298 to −99 bp. The −98 bp fragment resulted in background activity and was defined as *NIN* minimal promoter (*pNINmin*). GUS expression is shown relative to the value obtained for the *pNIN(−7):GUS* reporter construct (set to 1).

(C–F) Fine mapping of the upstream RE ('*CYC-RE*') via *NIN* promoter fragments fused to the 5′ end of *pNINmin:GUS*. GUS activity is shown relative to the value obtained for *pNINmin:GUS* (set to 1).

(C) A ~50 bp deletion series (*D1*–*D6*) delimited the position of the *CYC-RE* to the interval from −785 to −685 bp. Deletion constructs were tested in the background of a −298 to −99 bp deletion (dotted line). *D1* = −834 to −299 bp, *D2* = −785 to −299 bp, *D3* = −735 to −299 bp, *D4* = −685 to −299 bp, *D5* = −635 to −299 bp, *D6* = −579 to −299 bp.

(D) Analysis of overlapping promoter fragments (*B1*–*B4*) delimited the *CYC-RE* location to a 71 bp fragment (*B4*). *B1* = −735 to −615 bp, *B2* = −785 to −716 bp, *B3* = −785 to −615 bp, *B4* = −735 to −666 bp.

(E) Dissection of *B4* into three overlapping 36 bp fragments (*F1*–*F3*) identified *F2* as a minimal region containing the *CYC-RE* depicted in (F). *F1* = −735 to −701 bp, *F2* = −717 to −683 bp and *F3* = −700 to −666 bp.

(F) *CYC-RE* contains a palindromic sequence (*CYC-box*) which is essential for transactivation via CYCLOPS-DD. *CYC-RE*, five mutant versions (*M1-M5*) and a mutant variant of the entire palindrome (*mCYC-RE*) were analyzed as tandem repeat ('2x') fusions to *pNINmin:GUS*. Nucleotide sequences of *CYC-RE*, *mCYC-RE*, *M1-M5*, *1PAL1*, *mPAL*, *CYC-box* ('*PAL*' = palindrome) are depicted; the palindrome sequence is depicted in blue letters, mutated nucleotides are depicted in red. See also Figure S4.

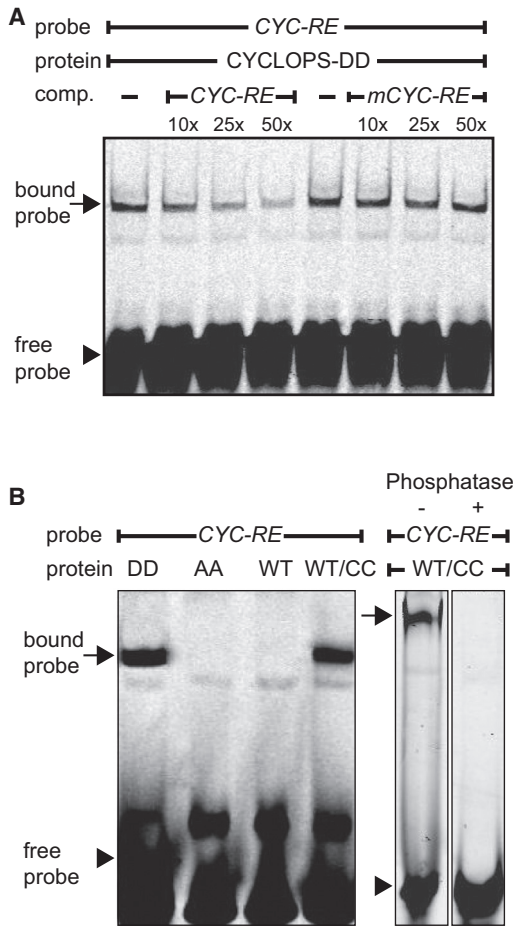


**Figure 3. CYCLOPS Binds the *NIN* Promoter in a Sequence-Specific and Phosphorylation-Dependent Manner**

(A) EMSA showing that CYCLOPS-DD has higher affinity to WT *CYC-RE* than to mutant *mCYC-RE* DNA. EMSA was performed with GST-CYCLOPS-DD (35 pmol), IR-labeled *CYC-RE* (0.1 pmol) as probe, and unlabeled competitor (comp.) DNA (*CYC-RE* or *mCYC-RE*) at 10-, 25- and 50-fold molar excess.

(B) CYCLOPS binds the *CYC-RE* in a phosphorylation-dependent manner. Left panel: Equal concentrations (35 pmol) of GST-CYCLOPS-DD (DD), GST-CYCLOPS-AA (AA), GST-CYCLOPS-WT (WT), or 40 pmol of Strep-CYCLOPS-WT protein purified after coexpression with 6xHis-CCaMK (WT/CC) were tested for binding to IR-labeled *CYC-RE* (0.1 pmol). Right panel: Untreated (–) and phosphatase treated (+) Strep-CYCLOPS-WT protein (20 pmol) purified after coexpression with 6xHis-CCaMK (WT/CC) was tested with IR-labeled *CYC-RE* (0.1 pmol) as probe. In (A) and (B), the position of specifically bound and free probe is indicated by an arrow and an arrowhead, respectively. Samples were resolved on 6% (A and B, right panel) or 4% (B, left panel) polyacrylamid gels. See also Figure S4.

## The CYCLOPS DNA-Binding Domain Binds the *CYC-RE* In Vitro

The delimitation of the $BD_{CYC}$ to aa 364–518 was substantiated by direct DNA-binding assays. In EMSAs, CYCLOPS-BD (aa 364–518) bound strongly to labeled *CYC-RE* (Figure 4D). The WT palindromic sequence (*1PAL1*, Figure 2F), but not the mutated palindrome (*1mPAL1*, Figure 2F), competed efficiently for the binding, thus not only demonstrating sequence specificity but narrowing down the DNA sequence sufficient for CYCLOPS' binding to the *CYC-box*. Sequence-specific DNA binding of CYCLOPS-BD was also confirmed by microscale thermophoresis (Figure 4E). Notably, CYCLOPS-DD-ΔBD (aa 1–366), lacking the deduced $BD_{CYC}$, did not show DNA-binding activity (Figures 4D and 4E). Taken together, these findings underscored that CYCLOPS-BD binds the *CYC-box* in a sequence-specific manner, matching the sequence specificity of CYCLOPS-DD.

## CYCLOPS-DD Transactivates *NIN* via the *CYC-RE* in *L. japonicus* Independently of *NSP1*, *NSP2*, and *NIN*

Our results so far are consistent with a model in which the phosphorylation of S50 and S154 leads to a structural change in CYCLOPS, which is associated with increased DNA-binding affinity and transactivation properties. The phosphomimetic replacements of both serine residues turn CYCLOPS into an autoactive transcription factor. A prediction from this model is that this autoactive version (CYCLOPS-DD) should induce symbiosis-related transcriptional activation and resultant phenotypic responses in *L. japonicus* roots. Indeed, expression of CYCLOPS-DD triggered strong and specific induction of the *2xCYC-RE:GUS* reporter only when containing the WT but not a mutant version of the palindrome (Figures 5A and 5C; Table S3), demonstrating that sequence specificity of the activation is retained in *L. japonicus*. This transactivation activity of CYCLOPS-DD was also detected in a *ccamk* mutant (Figure 5D). On the other hand, when CYCLOPS phosphorylation was stimulated by coexpression of autoactive CCaMK-T265D, strong induction of *2xCYC-RE:GUS* was detected, which was dependent on and correlated with CYCLOPS abundance since it was absent in the *cyclops-3* mutant and increased strongly when CYCLOPS-WT was overexpressed (Figures 5G, 5H, and 5J). This finding clearly implicated CYCLOPS as a key player in CCaMK-mediated *CYC-RE:GUS* activation. (Table S3).

To confirm that the endogenous *NIN* gene is a target of CYCLOPS-DD in *L. japonicus,* we employed real-time RT-PCR analysis on transgenic *ccamk-13* roots, constitutively expressing either *CYCLOPS-DD* or *CYCLOPS-AA* (Figure 6Q). Although both transgenes were expressed at similarly high levels, only in root systems transformed with *CYCLOPS-DD* transcription of *NIN* and of its target gene *NF-YA1* was activated (Figure 6Q). *GUS* gene-expression matching this pattern was also observed in roots of a transgenic *L. japonicus* $NIN_{pro}$*:GUS* reporter line transformed with $UB_{pro}$*:3xHA-CYCLOPS-WT*, *-DD*, *-AA*, or the empty vector control (data not shown).

As transcription factors can act in a combinatorial manner as heteromeric complexes, we also asked whether transactivation of *2xCYC-RE:GUS* by CYCLOPS-DD in *L. japonicus* depended on putative transcriptional regulators required for nodulation, such as the GRAS domain proteins NSP1, NSP2, and the transcription factor NIN, all of which have previously been positioned downstream of CCaMK (Marsh et al., 2007; Tirichine et al., 2006). Transformation of *nsp1, nsp2*, and *nin* mutant roots with $UB_{pro}$*:3xHA-gCYCLOPS-DD* and *2xCYC-RE:GUS* in all cases resulted in strong reporter expression, indicating that these transcriptional activators were dispensable for CYCLOPS-DD-mediated transactivation (Figures

S7D–S7F; Table S3). Consistent with this observation, CYCLOPS-DD-mediated *NIN* expression was equally detected in *ccamk*, *cyclops*, *nsp1*, and *nsp2* mutants (Figures S7A–S7C).

We conclude that CYCLOPS-DD acts as a transcriptional activator, which is sufficient to drive *2xCYC-RE:GUS*, $NIN_{pro}$*:GUS* and endogenous *NIN* expression in *L. japonicus*.

### The *2xCYC-RE:GUS* Reporter Is Activated in *L. japonicus* Roots after Inoculation with *M. loti*

We determined whether the identified CYCLOPS target *CYC-RE* was also activated in *L. japonicus* roots upon *M. loti* inoculation. Indeed, *2xCYC-RE:GUS* reporter expression but not a control reporter carrying the mutant palindrome was induced upon *M. loti* inoculation, indicating sequence-specific activation via *CYC-RE* during symbiosis signaling (Figures S6A and S6C; Table S4). This activation was dependent on *CYCLOPS* as the *M. loti*-triggered activation of *CYC-RE:GUS* was abolished in the *cyclops-3* mutant (Figure S6B).

### CYCLOPS-DD Induced Spontaneous Nodules Independently of CCaMK

Deregulated versions of CCaMK lead to spontaneous nodule organogenesis in the absence of rhizobia (Gleason et al., 2006; Tirichine et al., 2006). If CYCLOPS phosphorylation was indeed a key event in symbiotic signaling downstream of CCaMK, one prediction would be that CYCLOPS-DD expression leads to a symbiotic gain-of-function phenotype *in planta* independent of the presence of CCaMK. We transformed $CYC_{pro}$*:3xHA-gCYCLOPS-DD* into the *ccamk-3* (encoding a kinase-dead *CCaMK* mutant) and the *ccamk-13* (a *CCaMK*-null mutant carrying a premature stop codon) mutant backgrounds and cultivated the plants in the absence of rhizobia. Strikingly, CYCLOPS-DD triggered the spontaneous formation of root nodules with 30%–40% of transformed plants forming an average of 2–5 nodules per nodulated plant (Figure 6; Table S5). This effect was specifically observed on roots transformed with $CYC_{pro}$*:3xHA-gCYCLOPS-DD* and not on roots transformed with either the empty vector control, $CYC_{pro}$*:3xHA-gCYCLOPS-WT*, or other *CYCLOPS* mutant derivatives (Table S5). This observation indicated that CYCLOPS-DD was able to activate the nodule organogenesis program bypassing the requirement for CCaMK.

To genetically position *CYCLOPS-DD* relative to other genes required for nodule organogenesis, we transformed *L. japonicus* Gifu WT, *symrk-3, cyclops-3, nsp1-2*, *nsp2-2*, *nin-8*, and *cerberus-1* mutant roots with $CYC_{pro}$*:3xHA-gCYCLOPS-DD*. Spontaneous nodules were induced in the Gifu WT, *symrk-3*, *cyclops-3*, and *cerberus-1* mutants, whereas no nodules were formed on *nsp1-2*, *nsp2-2*, and *nin-8* mutant roots (Figure 6; Table S5). Spontaneous nodulation in the *symrk* mutant is consistent with the role of SYMRK in the activation of calcium spiking, which is upstream of CYCLOPS (Hayashi et al., 2010; Madsen et al., 2010). Furthermore, spontaneous nodules were formed in the *cerberus* mutant, which is in agreement with the positioning of *CERBERUS* on the infection related pathway, due to its role in infection thread formation (Madsen et al., 2010; Yano et al., 2009).

## DISCUSSION

### CCaMK/CYCLOPS Activate *NIN* Transcription upon Perception of Calcium Signals

The decoding of nuclear calcium signatures in multicellular organisms is involved in important cell fate decisions. In both animals and plants, the cell division program of specific cell types is triggered by nuclear calcium signatures in response to external stimuli (Clapham, 2007; Dodd et al., 2010). In plants, nuclear calcium spiking in root hair cells upon symbiotic stimulation was detected almost two decades ago (Ehrhardt et al., 1996) and CCaMK has emerged as the central regulator of symbiotic development (Singh and Parniske, 2012). However, the mechanism by and phosphorylation targets through which CCaMK mediates symbiotic development have been completely unclear.

Here we show that CYCLOPS is a DNA-binding transcriptional activator that connects phosphorylation by CCaMK directly to transcriptional gene regulation. Expression of autoactive CYCLOPS-DD in *ccamk* mutant roots induced the spontaneous development of root nodules in the absence of rhizobia, thus recapitulating the effect of deregulated CCaMK. This observation revealed that CYCLOPS phosphorylation is sufficient and additional CCaMK phosphorylation targets are dispensable for the initiation of nodule organogenesis by CCaMK pinpointing CYCLOPS as master regulator (Chan and Kyba, 2013) of root nodule organogenesis.

We propose a cascade of transcriptional regulation, which is initiated upon the activation of CCaMK by nuclear calcium signatures. Site-specific phosphorylation by CCaMK turns CYCLOPS into a transcriptional activator of the *NIN* gene. *NIN* induction alone can conceptually explain the spontaneous formation of lateral organs, as ectopic expression of *NIN,* which regulates *NF-YA1* and *NF-YB1* expression, induced the formation of abnormal lateral root organs partly resembling nodule primordia (Soyano et al., 2013). Based on accumulating evidence in legumes and in analogy to their mammalian homologs, a heterotrimeric NF-Y complex is believed to trigger entry into the cell division cycle (Laloum et al., 2013). Although ectopic *NIN* expression induced lateral organ formation, full-sized round-shaped nodules as mediated by CYCLOPS-DD were not observed (Soyano et al., 2013). This may indicate that the precise spatiotemporal regulation of *NIN* is important for proper organogenesis, possibly achieved through a combination of local calcium signaling and *CYCLOPS* gene-expression pattern. It is also possible that alternative CYCLOPS target genes beside *NIN* are required for nodule formation. Our data demonstrate that CYCLOPS-DD is sufficient to trigger nodule development (Figure 6). However, autoactive CCaMK was previously shown to also form nodules (albeit with reduced frequency) in the *cyclops* mutant. Moreover, *L. japonicus cyclops* and *M. truncatula* mutants defective for the *CYCLOPS* ortholog *IPD3* produced uninfected nodule primordia and nodules, respectively, upon rhizobia inoculation (Horváth et al., 2011; Ovchinnikova et al., 2011; Yano et al., 2008). Genetic redundancy at the hierarchical level of *CYCLOPS* is likely to account for this discrepancy. Possibly, yet-to-be-identified phosphorylation targets of CCaMK are able to, at least partially, substitute for the loss of CYCLOPS in the organogenesis, but not the infection pathway. *NSP1* and *NSP2* did not significantly contribute to

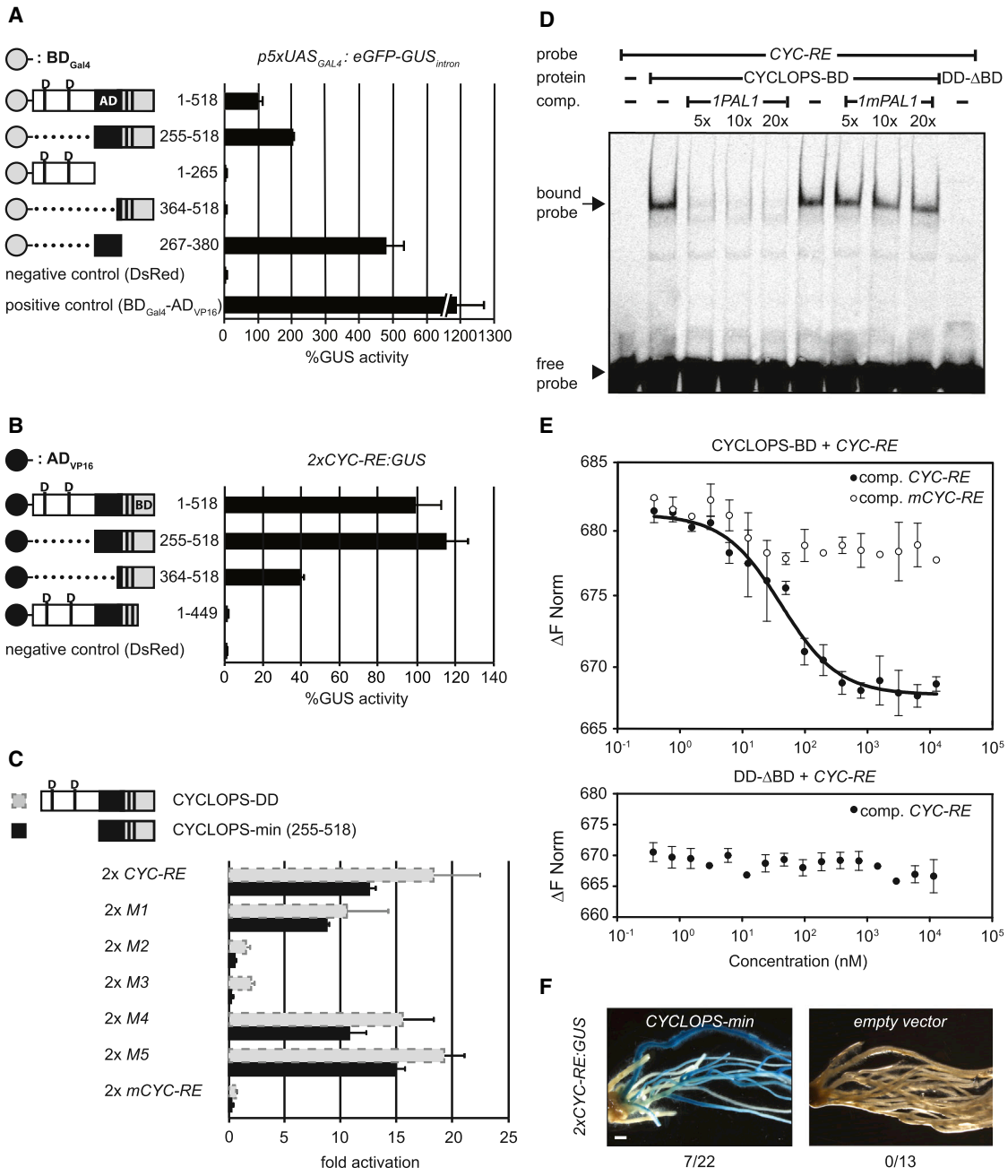


**Figure 4. CYCLOPS Is a Modular DNA-Binding Transcriptional Activator**

(A and B) Mapping of the CYCLOPS transcriptional activation domain (AD, in black) and DNA-binding domain (BD, in gray). *BD$_{Gal4}$-* or *AD$_{VP16}$-3xHA-CYCLOPS-DD* and truncated versions were coexpressed with the reporters *p5xUAS$_{Gal4}$:eGFP-GUS$_{intron}$* (A) or *2xCYC-RE:GUS* (B) in *N. benthamiana* leaves. T-DNAs encoding a *BD$_{Gal4}$-AD$_{VP16}$* fusion (A) or *DsRed* (A and B) were used as positive and negative controls, respectively. All constructs were constitutively expressed under control of the *35S* promoter. Data are mean values from three biological replicates and represented as percentage of GUS activity relative to BD$_{Gal4}$- (A) or AD$_{VP16}$-3xHA-CYCLOPS-DD (B), set to 100%. BD$_{Gal4}$ is depicted as gray circle in (A), AD$_{VP16}$ is depicted as black circle in (B).

(C) A minimal CYCLOPS version (aa 256–518) comprising both AD$_{CYC}$ and BD$_{CYC}$ is sufficient to mediate transcriptional activation via the *CYC-RE* in *N. benthamiana* leaves. *3xHA-CYCLOPS-min* was coexpressed with *2xCYC-RE:GUS*, or the indicated reporter mutant versions. GUS expression is shown relative to the value obtained with the *pNINmin:GUS* reporter (set to 1). Transactivation activity is compared between 3xHA-CYCLOPS-min (black bars) and 3xHA-CYCLOPS-DD (gray bars; values from Figure 2F). The graph shows mean values and standard deviations calculated from three biological replicates.

(D) CYCLOPS-BD (aa 364–518), containing the DNA-binding domain of CYCLOPS (BD$_{CYC}$), specifically binds to the *CYC-box* within the *CYC-RE* in vitro. GST-CYCLOPS-BD and a C-terminal truncation lacking the BD$_{CYC}$ (GST-CYCLOPS-DD-ΔBD; "DD-ΔBD", aa 1–449) (75 pmol each) were probed with IR-labeled *CYC-RE* (0.1 pmol) by EMSA. Unlabeled competitor DNA carrying either the wild-type (*1PAL1*) or mutated palindrome (*1mPAL1*) (Figure 2F), was used in 5-, 10- and 20-fold molar excess. The arrows and the arrowhead indicate position of specifically bound and free probe, respectively. Samples were resolved on a 6% polyacrylamid gel.

*(legend continued on next page)*

endogenous *NIN* or *CYC-RE:GUS* activation by CYCLOPS-DD (Figure S7). Therefore, the absence of CYCLOPS-DD-induced spontaneous nodules in *nsp* mutants is unlikely a consequence of altered *NIN* activation, and thus the NSPs presumably act downstream or in parallel pathways.

### CYCLOPS Carries a Noncanonical DNA-Binding Domain

We identified a modular domain structure in CYCLOPS comprising functionally separable DNA binding and activation domains (Figure 4). This structure is typical for eukaryotic DNA-binding transcriptional activators. However, by interrogating a range of specific databases (see Experimental Procedures) we were unsuccessful in detecting similarity to canonical DNA-binding motifs. Therefore we conclude that CYCLOPS represents a hitherto uncharacterized type of DNA-binding protein.

### The CYCLOPS AD Contains a Peptide Stretch with Predicted Intrinsic Disorder

The experimentally determined maximal extension of the CYCLOPS AD (aa 267–380) carries a conserved serine/threonine-rich stretch (Figure S1B), which is located in an intrinsically disordered region as predicted by DISPHOS (see Experimental Procedures). Thus, the CYCLOPS AD region shares two features with characterized transcriptional activation domains (Liu et al., 2006) and in analogy may become structured by a conformational change upon phosphorylation at S50 and S154 and/or upon interaction with the basal transcriptional machinery (Figure 7).

### The N-Terminal Half of CYCLOPS Functions as a Negative Regulatory Domain

Our domain analysis confined the transcriptional AD and the DNA-BD of CYCLOPS to the C-terminal half (aa 267–518) (Figure 4). CYCLOPS-min composed of the C-terminal AD and BD domains fully transactivated via the *CYC-RE*, displaying the same sequence specificity as CYCLOPS full length (Figure 4C). Since the N terminus is not required and its removal leads to an active transcription factor, we conclude that it acts as negative regulatory domain. Interestingly, although CYCLOPS-min was able to trigger *CYC-RE:GUS* activation in *L. japonicus* roots (Figure 4F), it was unable to trigger *NINpro:GUS* activity (not shown) and did not induce spontaneous nodules (Table S5). These results indicate that CYCLOPS' N terminus is required for spontaneous *NIN* activation and nodule organogenesis.

### The Consequences of CYCLOPS Phosphorylation

CYCLOPS phosphorylation by CCaMK leads to transcriptional activation of the *NIN* promoter (Figure 2A). This effect can be mimicked by phosphomimetic versions of the two CCaMK substrate residues S50 and S154, whereas phosphoablative versions are completely blocked in this activity (Figures 2A and 6Q). Since both regulatory serines are located in the N-terminal region, which is inhibiting CYCLOPS' activity (Figure 4C), we postulate that the "DD" replacement (and by inference, phosphorylation) induces a conformational change that releases the DNA-binding and transcriptional AD from autoinhibition by the N terminus (Figure 7). This model is further supported by the strong effect of CYCLOPS phosphorylation on DNA-binding activity (Figure 3B).

Our data indicate that the hydroxyl groups of S50 and S154 play an important role in allowing the N terminus to adopt a permissive conformation. Homodimerization activity was detected by FLIM-FRET analysis for all CYCLOPS phosphosite variants (Figures 1G–1I). However, a stronger FRET was observed solely for CYCLOPS-DD. This argues for an altered conformation of the dimer that might explain a higher affinity to DNA. It is possible that conformational changes induced by CYCLOPS phosphorylation may alter the geometry between the DNA-binding sites of the CYCLOPS monomers, thus influencing affinity to palindromic targets, a principle also found for other transcription factors (Schumacher et al., 1995).

### Decoding of Symbiotic Calcium Oscillations by the CCaMK/CYCLOPS Complex Provides a Paradigm in Nuclear Calcium-based Signal Transduction

The closest homolog of CCaMK in vertebrates is calcium/calmodulin-dependent kinase II (CaMKII) involved in the decoding of calcium spiking in neuronal and cardiac signaling (Stratton et al., 2013). Although sequence related, there are some fundamental differences in their mode of action (Hudmon and Schulman, 2002; Sathyanarayanan et al., 2001). In addition, CaMKII isoforms exist that localize to both compartments the cytosol and the nucleus (Buchthal et al., 2012). The only known CaMKII pathway involved in direct transcriptional regulation is the CaMKII/MeCP2 (methyl-CpG-binding protein) pathway (Buchthal et al., 2012; Wayman et al., 2008), in which nuclear calcium-stimulated CaMKII activity phosphorylates MeCP2, a genome-wide transcriptional repressor or activator. However, the mechanism of action of MeCP2, which binds to methylated cytosines, is very different from the one discovered here.

Among characterized CaMKs, only CaMKIV, acting in the CAMKIV/CREB/CBP (cAMP-response element-binding/CREB-binding protein) "CCC" pathway, is exclusively localized in the nucleus (Wayman et al., 2008). Activated CaMKIV phosphorylates the transcription factor CREB and the coactivator CBP,

(E) Microscale thermophoresis demonstrating that GST-CYCLOPS-BD specifically binds to the *CYC-RE* in vitro (upper panel), whereas GST-CYCLOPS-DD-ΔBD (DD- ΔBD) is impaired (lower panel). Upper panel: Binding of GST-CYCLOPS-BD to labeled *CYC-RE* was competed by addition of unlabeled WT *CYC-RE* (black circles) or mutated *mCYC-RE* (white circles) in increasing concentrations. Lower panel: The reaction of DD-ΔBD with labeled *CYC-RE* showed no change in thermophoresis values when unlabeled *CYC-RE* was added in increasing concentrations, indicating an impairment in *CYC-RE* binding. Average thermophoresis values and standard deviations of three experimental replicates are shown. MST was performed with 25 nM labeled *CYC-RE* and 1.3 μM GST-CYCLOPS-BD, or GST-CYCLOPS-DD-ΔBD, respectively. Comp.: competitor probe.

(F) The *2xCYC-RE:GUS* reporter is induced in *L. japonicus cyclops-3* mutant roots cotransformed with $UB_{pro}$*3xHA-cCYCLOPS-min*, but not in roots cotransformed with the empty vector. Blue staining indicates GUS reporter activity. Numbers indicate GUS positive root systems per total stained root systems. See also Figure S5.

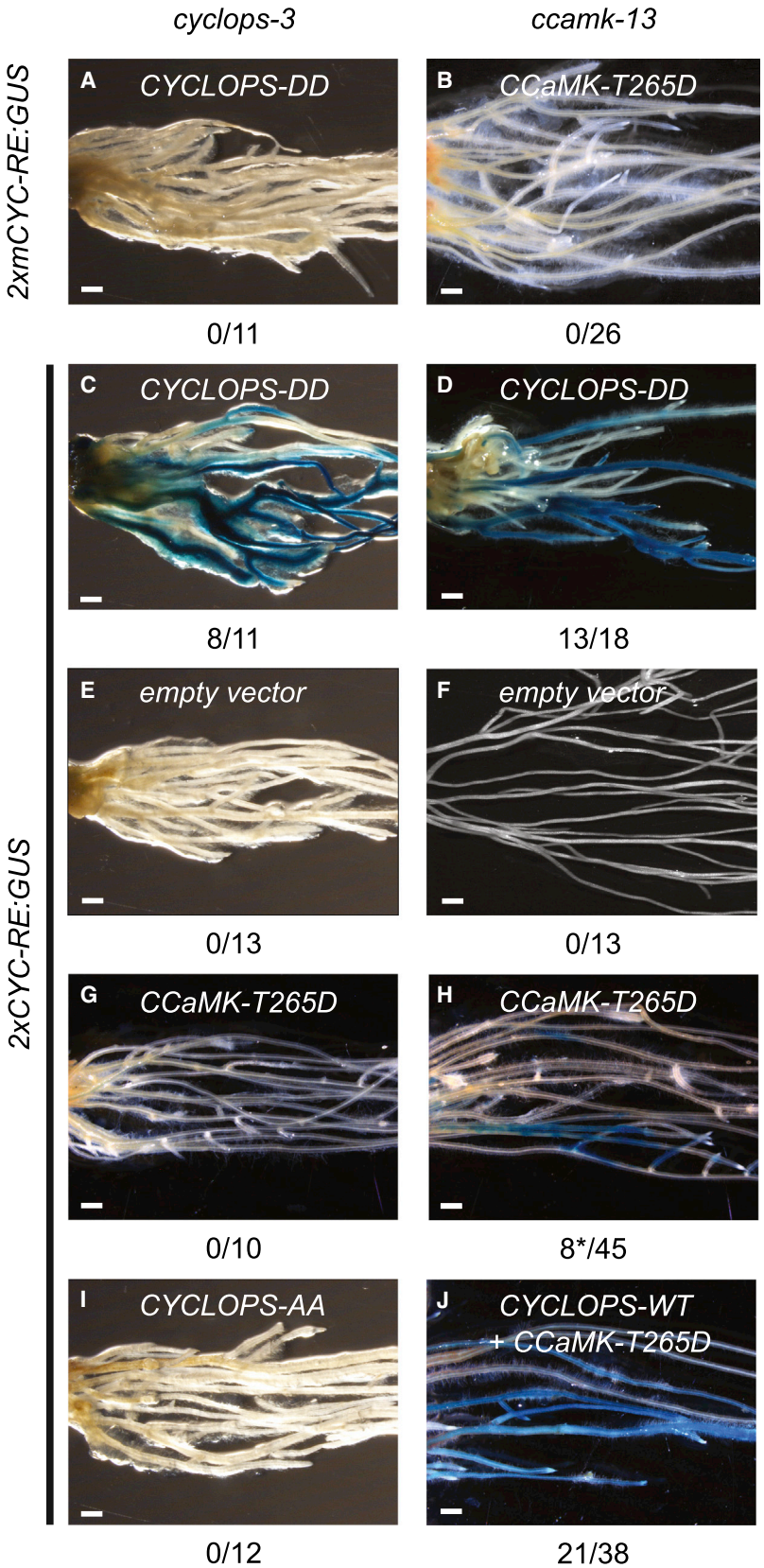


**Figure 5. CYCLOPS-DD Activates the *CYC-RE* Independently of CCaMK in *L. japonicus* Roots**

(A–J) Transactivation assays in *L. japonicus cyclops-3* and *ccamk-13* mutant roots cotransformed with the reporter constructs indicated on the left and $UB_{pro}$*3xHA-gCYCLOPS-WT*, *-DD*, *-AA*, $UB_{pro}$*cCCaMK-T265D*, or the empty vector (negative control). *2xCYC-RE:GUS* is activated in *cyclops-3* and *ccamk-13* roots cotransformed with *3xHA-gCYCLOPS-DD* (C and D), but not with the empty vector control (E and F). *2xmCYC-RE:GUS* was not induced in *cyclops-3* roots cotransformed with *3xHA-gCYCLOPS-DD* (A) or in *ccamk-13* roots cotransformed with *cCCaMK-T265D* (B). Neither expression of *cCCaMK-T265D* (G), or *3xHA-gCYCLOPS-AA* (I) induced the *2xCYC-RE:GUS* reporter in *cyclops-3* roots. Faint GUS staining was occasionally observed in *ccamk-13* roots cotransformed with *2xCYC-RE:GUS* and *cCCaMK-T265D* (H), whereas additional ectopic expression of *3xHA-gCYCLOPS-WT* led to a strong induction (J). Reporter activation is visualized by blue staining resulting from GUS activity. Numbers indicate GUS positive roots per total stained root systems. *: weak GUS staining. Bars: 1 mm. See also Figure S6.

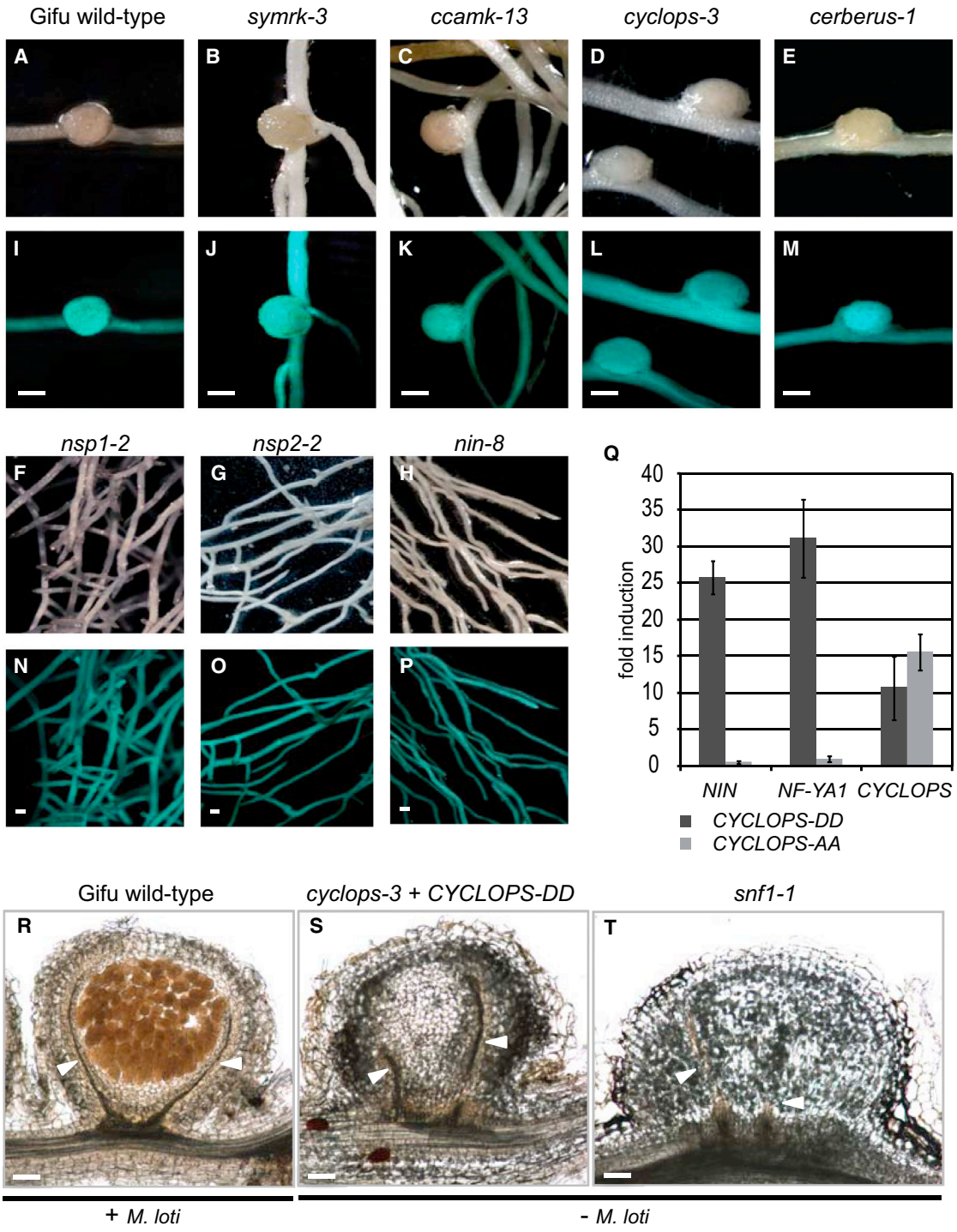


**Figure 6. CYCLOPS-DD Induces the Formation of Spontaneous Nodules in the Absence of Rhizobia, Independently of *CCaMK* and Upregulates *NIN* and *NF-YA1* Expression**

(A–P and R–T) Spontaneous root nodule development induced in roots transformed with $CYC_{pro}$*3xHA-gCYCLOPS-DD* was observed on transgenic roots of the *L. japonicus* Gifu WT (A and I) and *symrk-3* (B and J) *ccamk-13* (C and K) *cyclops-3* (D and L) and *cerberus-1* (E and M) mutants, but not on those of *nsp1-2* (F and N), *nsp2-2* (G and O) and *nin-8* (H and P) mutants. Spontaneous nodule formation was evaluated on transgenic mutant roots (A–P) or untransformed *snf1-1* roots (T) 8 weeks post transformation and cultivation in the absence of rhizobia. Infected nodules (R) were collected from 8 weeks old untransformed Gifu-wild-type roots 1 month post *M. loti-Ds*Red inoculation. CYCLOPS-DD induced spontaneous nodules (S) are equivalent to those formed in the *snf1-1* mutant (T), featuring peripheral vascular bundles (white arrowheads), which is a hallmark of rhizobia-induced root nodules (R). Note the absence of rhizobia in cortical cells in (S) and (T). Brightfield images: (A–H); (R–T) (longitudinal 40 μm sections). Images of GFP fluorescence demonstrate expression of the transformation

*(legend continued on next page)*

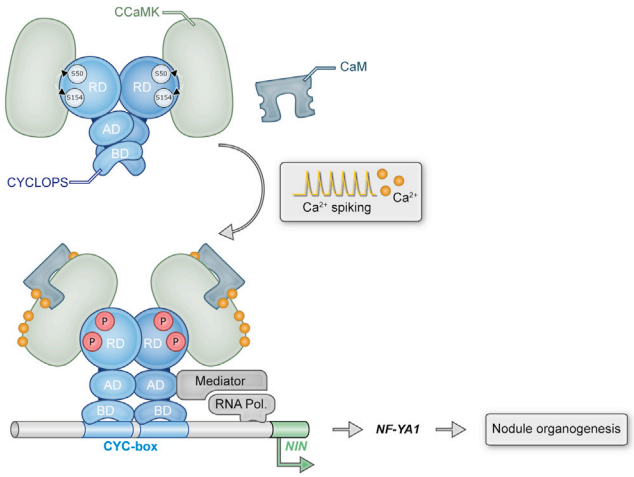


**Figure 7. Proposed Function of the CCaMK/CYCLOPS Complex in the Decoding of Nuclear Calcium Signatures Leading to Root Nodule Development**

CCaMK and CYCLOPS form a preassembled inactive and autoinhibited complex in root cell nuclei in which CYCLOPS is present as a dimer. Upon initiation of symbiotic nuclear calcium spiking, CCaMK is activated by $Ca^{2+}$/Calmodulin (CaM) and phosphorylates (P) CYCLOPS at S50 and S154. CYCLOPS phosphorylation induces a conformational change releasing the DNA-binding (BD) domain from autoinhibition exerted by the N-terminal regulatory domain (RD). Consequently, CYCLOPS binds the *CYC-box* in the *NIN* promoter and recruits the basal transcription machinery via its activation domain (AD), inducing *NIN* expression. Deregulated CYCLOPS is sufficient to reinitiate the cell cycle in differentiated cortical cells resulting in nodule organogenesis. This involves the cascade of transcriptional activation of *NIN* and *NF-YA1* in hierarchical succession. RNA-Pol.: RNA Polymerase II.

which are both required for calcium-induced CREB-dependent gene expression (Wayman et al., 2008). Mechanistically, the CCC pathway is the closest known system to CCaMK/CYCLOPS for the decoding of nuclear calcium signatures. However, in contrast to the CCC pathway there are no additional CCaMK-phosphorylated coactivators required for transactivation by CYCLOPS. Therefore, we report a most parsimonious mechanism of nuclear calcium signal transduction leading to stimulus-specific gene expression. The CCaMK/CYCLOPS pair and the CCC system are phylogenetically restricted to plants (Wang et al., 2010) and metazoans (Tombes et al., 2003), respectively. Apparently, animal and plant cells have convergently evolved independent nuclear kinase-substrate pairs to mediate calcium stimulated transcriptional regulation.

## EXPERIMENTAL PROCEDURES

### FLIM-FRET Analysis

FLIM-FRET analysis was performed on transformed *N. benthamiana* leaf discs essentially as described (Bayle et al., 2008). Measurements were done on a Leica SP5 equipped with a pulsed multiphoton laser (Spectra Physics) and the Becker and Hickl FLIM-FRET package. One-way ANOVA and Tukey's HSD test were used for statistical analysis.

### Fluorimetric GUS Assay

Two infiltrated *N. benthamiana* leaf discs per sample were harvested 60 hpi and frozen in liquid nitrogen. Leaf tissue was ground with a tissue lyser (QIAGEN), and protein was extracted with extraction buffer (50 mM $NaPO_4$, pH 7.0, 10 mM EDTA, 10 mM β-ME, 0.1% N-Lauryl-Sarcosine, 0.1% Triton X-100, complete protease inhibitor, [Roche]). Extracts were centrifuged (10.000x *g*, 15 min, 4°C) and the supernatant was used for GUS activity measurement as described (Jefferson et al., 1987) with 4-methylumbelliferyl β-D-glucuronide as substrate and 4-methyl-umbelliferon (both from Roth) as standard. Samples were measured in a plate reader (Tecan) at 360 nm excitation and 465 nm emission. Proteins were quantified using Bradford assay (Bio-Rad). Mean values and standard deviations were determined from three biological replicates.

### Electrophoretic Mobility Shift Assay

Binding reactions contained 10 mM Tris-HCl (pH 7.5), 50 mM KCl, 1 mM DTT, 2.5% (vol/vol) glycerol, 5 mM $MgCl_2$, 25–50 ng/μL poly (dI•dC), 0.05% Nonidet P-40, 0.2 mM EDTA, 100 fmol 5′ DY682 labeled DNA, competitor DNA in 5- to 50-fold molar excess and 35–75 pmol CYCLOPS protein (competitor DNA and protein concentrations are given in figure legends). To increase DNA-binding specificity, EMSAs shown in Figures 3A and 4D were performed in the presence of 150 mM and 250 mM KCl, respectively. Binding reactions were incubated at room temperature for 20 min. Reactions were resolved on 4% or 6% native polyacrylamide gels (see figure legends) and DY682 labeled DNA was visualized with the Odyssey system (LI-COR Biosciences). Complementary pairs of labeled (5′DY682) and unlabeled oligonucleotide probes are listed in Table S6.

### Protein Expression and Purification

Expression of all proteins was induced in *E. coli* Rosetta pLaqI (Novagen) for 4 hr at 28°C by addition of 0.5–1 mM IPTG. Protein purification was performed essentially as described by the protocol of the resin manufacturer. CCaMK was purified via CaM-Sepharose beads (GE-Healthcare), and was desalted via PD10 desalting column (GE-Healthcare) using buffer containing 25 mM Tris and 10 mM β-ME (pH 7.6). Expression and purification of 6xHis-CYCLOPS was performed as described (Yano et al., 2008). For EMSA or microscale thermophoresis analysis, GST-CYCLOPS, GST-CYCLOPS-AA, GST-CYCLOPS-DD, GST-CYCLOPS-BD, and GST-CYCLOPS-DDΔBD were purified with Glutathione HiCap Matrix (QIAGEN) using modified buffer conditions (binding and wash buffer: 20 mM PIPES, 200 mM KCl, 1 mM DTT, pH 7.9; for protein elution the wash buffer was supplemented with 50 mM reduced L-Glutathione). StrepII-tagged CYCLOPS protein was coexpressed with 6xHis-CCaMK and purified via Strep-Tactin-Sepharose (IBA) according to the manufacturer's manual but using 50 mM Tris, pH 7.8. Protein concentration was determined by the Bradford Method (Bio-Rad), using BSA (Sigma) as a standard, and protein purity was analyzed by SDS-PAGE and Coomassie staining of the gel.

### Microscale Thermophoresis

Specific binding between GST-CYCLOPS-BD or GST-CYCLOPS-ΔBD-DD protein and *CYC-RE* DNA probe was measured by the microscale thermophoresis method as described (Jerabek-Willemsen et al., 2011). Binding experiments were performed with 25 nM Cy5 labeled *CYC-RE* and 1.3 μM GST-CYCLOPS-BD or GST-CYCLOPS-DD-ΔBD protein. Increasing amounts (from 381 pM to 12.5 μM) of unlabeled competitor probe (*CYC-RE*, or mutated *mCYC-RE*) were added. Binding reactions were carried out in buffer containing 20 mM Tris pH 7.4, 150 mM NaCl, 10 mM $MgCl_2$, and 0.05% Tween. Samples

marker: I–P. Bars: 0.5 mm in A–P, 0.1 mm in R–T. In Q, real-time RT-PCR analysis of *NIN*, *NF-YA1*, and *CYCLOPS* expression in *ccamk-13* roots transformed with $UB_{pro}$*:3xHA-gCYCLOPS-DD*, *-AA*, or the empty vector control. Expression analysis was performed 4 weeks post transformation. Relative expression was normalized to the reference genes *EF-1alpha* and *UBIQUITIN*. Fold induction levels were calculated relative to the expression obtained from hairy roots transformed with the empty vector control (expression level = 1). Graph represents mean values and standard deviations obtained from the analysis of three biological replicates. See also Figure S7.

were loaded into NT.115 standard capillaries (Nanotemper Technologies) and thermophoresis was carried out at 25°C, 80% LED, and 40% IR-laser power using the Monolith NT.115 (Nanotemper Technologies). Data analysis was performed with Nanotemper Analysis software v.1.2.101. Average thermophoresis values and standard deviations were calculated from three independent measurements and curve fitting was calculated using SigmaPlot 11.0 software (Systat software).

## SUPPLEMENTAL INFORMATION

Supplemental Information includes seven figures, seven tables, Supplemental Experimental Procedures, and Supplemental References and can be found with this article online at http://dx.doi.org/10.1016/j.chom.2014.01.011.

## ACKNOWLEDGMENTS

We thank Andreas Binder (University of Munich, Germany) for preparing Figure 7, Riyaz A. Bhat (Solazyme, San Francisco, USA) for providing the FLIM-FRET vectors, Makoto Hayashi (National Institute of Agrobiological Sciences, Tsukuba, Japan) for *pNIN:GUS*, Remko Offringa (Leiden University, Netherlands) for plasmid pSDM7006, Jens Stougaard (Aarhus University, Denmark) for *L. japonicus ccamk-13* seeds, Trevor Wang (John Innes Centre, UK) for *L. japonicus nsp1-1* seeds, and Andreas Niebel (LIPM, France) for the ChIP protocol and advice on the technique. This work was funded by a grant from the German Research Foundation (DFG) to M.P. within Research Unit FOR 964 "Calcium signaling via protein phosphorylation in plant model cell types during environmental stress adaptation."

Received: July 5, 2013
Revised: November 30, 2013
Accepted: January 24, 2014
Published: February 12, 2014

## REFERENCES

Bayle, V., Nussaume, L., and Bhat, R.A. (2008). Combination of novel green fluorescent protein mutant TSapphire and DsRed variant mOrange to set up a versatile *in planta* FRET-FLIM assay. Plant Physiol. *148*, 51–60.

Bootman, M.D., Fearnley, C., Smyrnias, I., MacDonald, F., and Roderick, H.L. (2009). An update on nuclear calcium signalling. J. Cell Sci. *122*, 2337–2350.

Buchthal, B., Lau, D., Weiss, U., Weislogel, J.M., and Bading, H. (2012). Nuclear calcium signaling controls methyl-CpG-binding protein 2 (MeCP2) phosphorylation on serine 421 following synaptic activity. J. Biol. Chem. *287*, 30967–30974.

Chan, S.S., and Kyba, M. (2013). What is a Master Regulator? J. Stem Cell. Res. Ther. *3*, e114.

Clapham, D.E. (2007). Calcium signaling. Cell *131*, 1047–1058.

Conaway, R.C., Sato, S., Tomomori-Sato, C., Yao, T., and Conaway, J.W. (2005). The mammalian Mediator complex and its role in transcriptional regulation. Trends Biochem. Sci. *30*, 250–255.

Dodd, A.N., Kudla, J., and Sanders, D. (2010). The language of calcium signaling. Annu. Rev. Plant Biol. *61*, 593–620.

Ehrhardt, D.W., Wais, R., and Long, S.R. (1996). Calcium spiking in plant root hairs responding to *Rhizobium* nodulation signals. Cell *85*, 673–681.

Gleason, C., Chaudhuri, S., Yang, T., Muñoz, A., Poovaiah, B.W., and Oldroyd, G.E. (2006). Nodulation independent of rhizobia induced by a calcium-activated kinase lacking autoinhibition. Nature *441*, 1149–1152.

Gutjahr, C., and Parniske, M. (2013). Cell and developmental biology of arbuscular mycorrhiza symbiosis. Annu. Rev. Cell Dev. Biol. *29*, 593–617.

Hayashi, T., Banba, M., Shimoda, Y., Kouchi, H., Hayashi, M., and Imaizumi-Anraku, H. (2010). A dominant function of CCaMK in intracellular accommodation of bacterial and fungal endosymbionts. Plant J. *63*, 141–154.

Horváth, B., Yeun, L.H., Domonkos, A., Halász, G., Gobbato, E., Ayaydin, F., Miró, K., Hirsch, S., Sun, J., Tadege, M., et al. (2011). *Medicago truncatula IPD3* is a member of the common symbiotic signaling pathway required for rhizobial and mycorrhizal symbioses. Mol. Plant Microbe Interact. *24*, 1345–1358.

Hudmon, A., and Schulman, H. (2002). Neuronal $Ca^{2+}$/calmodulin-dependent protein kinase II: the role of structure and autoregulation in cellular function. Annu. Rev. Biochem. *71*, 473–510.

Jefferson, R.A., Kavanagh, T.A., and Bevan, M.W. (1987). GUS fusions: beta-glucuronidase as a sensitive and versatile gene fusion marker in higher plants. EMBO J. *6*, 3901–3907.

Jerabek-Willemsen, M., Wienken, C.J., Braun, D., Baaske, P., and Duhr, S. (2011). Molecular interaction studies using microscale thermophoresis. Assay Drug Dev. Technol. *9*, 342–353.

Kaló, P., Gleason, C., Edwards, A., Marsh, J., Mitra, R.M., Hirsch, S., Jakab, J., Sims, S., Long, S.R., Rogers, J., et al. (2005). Nodulation signaling in legumes requires NSP2, a member of the GRAS family of transcriptional regulators. Science *308*, 1786–1789.

Laloum, T., De Mita, S., Gamas, P., Baudin, M., and Niebel, A. (2013). CCAAT-box binding transcription factors in plants: Y so many? Trends Plant Sci. *18*, 157–166.

Lévy, J., Bres, C., Geurts, R., Chalhoub, B., Kulikova, O., Duc, G., Journet, E.P., Ané, J.M., Lauber, E., Bisseling, T., et al. (2004). A putative $Ca^{2+}$ and calmodulin-dependent protein kinase required for bacterial and fungal symbioses. Science *303*, 1361–1364.

Liu, J., Perumal, N.B., Oldfield, C.J., Su, E.W., Uversky, V.N., and Dunker, A.K. (2006). Intrinsic disorder in transcription factors. Biochemistry *45*, 6873–6888.

Madsen, L.H., Tirichine, L., Jurkiewicz, A., Sullivan, J.T., Heckmann, A.B., Bek, A.S., Ronson, C.W., James, E.K., and Stougaard, J. (2010). The molecular network governing nodule organogenesis and infection in the model legume *Lotus japonicus*. Nat. Commun. *1*, 10.

Marsh, J.F., Rakocevic, A., Mitra, R.M., Brocard, L., Sun, J., Eschstruth, A., Long, S.R., Schultze, M., Ratet, P., and Oldroyd, G.E. (2007). *Medicago truncatula NIN* is essential for rhizobial-independent nodule organogenesis induced by autoactive calcium/calmodulin-dependent protein kinase. Plant Physiol. *144*, 324–335.

Mitra, R.M., Gleason, C.A., Edwards, A., Hadfield, J., Downie, J.A., Oldroyd, G.E., and Long, S.R. (2004). A $Ca^{2+}$/calmodulin-dependent protein kinase required for symbiotic nodule development: Gene identification by transcript-based cloning. Proc. Natl. Acad. Sci. USA *101*, 4701–4705.

Miwa, H., Sun, J., Oldroyd, G.E.D., and Downie, J.A. (2006). Analysis of calcium spiking using a cameleon calcium sensor reveals that nodulation gene expression is regulated by calcium spike number and the developmental status of the cell. Plant J. *48*, 883–894.

Oldroyd, G.E.D. (2013). Speak, friend, and enter: signalling systems that promote beneficial symbiotic associations in plants. Nat. Rev. Microbiol. *11*, 252–263.

Ovchinnikova, E., Journet, E.P., Chabaud, M., Cosson, V., Ratet, P., Duc, G., Fedorova, E., Liu, W., den Camp, R.O., Zhukov, V., et al. (2011). *IPD3* controls the formation of nitrogen-fixing symbiosomes in pea and *Medicago Spp*. Mol. Plant Microbe Interact. *24*, 1333–1344.

Sathyanarayanan, P.V., Siems, W.F., Jones, J.P., and Poovaiah, B.W. (2001). Calcium-stimulated autophosphorylation site of plant chimeric calcium/calmodulin-dependent protein kinase. J. Biol. Chem. *276*, 32940–32947.

Schauser, L., Roussis, A., Stiller, J., and Stougaard, J. (1999). A plant regulator controlling development of symbiotic root nodules. Nature *402*, 191–195.

Schumacher, M.A., Choi, K.Y., Lu, F., Zalkin, H., and Brennan, R.G. (1995). Mechanism of corepressor-mediated specific DNA binding by the purine repressor. Cell *83*, 147–155.

Singh, S., and Parniske, M. (2012). Activation of calcium- and calmodulin-dependent protein kinase (CCaMK), the central regulator of plant root endosymbiosis. Curr. Opin. Plant Biol. *15*, 444–453.

Smit, P., Raedts, J., Portyanko, V., Debellé, F., Gough, C., Bisseling, T., and Geurts, R. (2005). NSP1 of the GRAS protein family is essential for rhizobial Nod factor-induced transcription. Science *308*, 1789–1791.

Soyano, T., Kouchi, H., Hirota, A., and Hayashi, M. (2013). Nodule inception directly targets NF-Y subunit genes to regulate essential processes of root nodule development in *Lotus japonicus*. PLoS Genet. *9*, e1003352.

Stratton, M.M., Chao, L.H., Schulman, H., and Kuriyan, J. (2013). Structural studies on the regulation of $Ca^{2+}$/calmodulin dependent protein kinase II. Curr. Opin. Struct. Biol.

Swainsbury, D.J., Zhou, L., Oldroyd, G.E., and Bornemann, S. (2012). Calcium ion binding properties of *Medicago truncatula* calcium/calmodulin-dependent protein kinase. Biochemistry *51*, 6895–6907.

Tirichine, L., Imaizumi-Anraku, H., Yoshida, S., Murakami, Y., Madsen, L.H., Miwa, H., Nakagawa, T., Sandal, N., Albrektsen, A.S., Kawaguchi, M., et al. (2006). Deregulation of a $Ca^{2+}$/calmodulin-dependent kinase leads to spontaneous nodule development. Nature *441*, 1153–1156.

Tombes, R.M., Faison, M.O., and Turbeville, J.M. (2003). Organization and evolution of multifunctional Ca(2+)/CaM-dependent protein kinase genes. Gene *322*, 17–31.

Wang, B., Yeun, L.H., Xue, J.Y., Liu, Y., Ané, J.M., and Qiu, Y.L. (2010). Presence of three mycorrhizal genes in the common ancestor of land plants suggests a key role of mycorrhizas in the colonization of land by plants. New Phytol. *186*, 514–525.

Wayman, G.A., Lee, Y.S., Tokumitsu, H., Silva, A.J., and Soderling, T.R. (2008). Calmodulin-kinases: modulators of neuronal development and plasticity. Neuron *59*, 914–931.

Yano, K., Shibata, S., Chen, W.L., Sato, S., Kaneko, T., Jurkiewicz, A., Sandal, N., Banba, M., Imaizumi-Anraku, H., Kojima, T., et al. (2009). CERBERUS, a novel U-box protein containing WD-40 repeats, is required for formation of the infection thread and nodule development in the legume-Rhizobium symbiosis. Plant J. *60*, 168–180.

Yano, K., Yoshida, S., Müller, J., Singh, S., Banba, M., Vickers, K., Markmann, K., White, C., Schuller, B., Sato, S., et al. (2008). CYCLOPS, a mediator of symbiotic intracellular accommodation. Proc. Natl. Acad. Sci. USA *105*, 20540–20545.